

Test and Theory of Electrodynamic Bearings Coupled to Active Magnetic Dampers

*Original*

Test and Theory of Electrodynamic Bearings Coupled to Active Magnetic Dampers / Impinna, Fabrizio; GIRARDELLO DETONI, Joaquim; Tonoli, Andrea; Amati, Nicola. - ELETTRONICO. - 14:(2014), pp. 263-268. ( 14th International Symposium on Magnetic Bearings Linz, Austria 11-14 August 2014).

*Availability:*

This version is available at: 11583/2561348 since:

*Publisher:*

*Published*

DOI:

*Terms of use:*

This article is made available under terms and conditions as specified in the corresponding bibliographic description in the repository

*Publisher copyright*

(Article begins on next page)

# Test and theory of electrodynamic bearings coupled to active magnetic dampers

Fabrizio Impinna, Joaquim G. Detoni, Andrea Tonoli, Nicola Amati, Maria Pina Piccolo

Department of Mechanical and Aerospace Engineering, Mechatronics Laboratory,  
Politecnico di Torino, Corso Duca degli Abruzzi, 24, 10129 Torino

**Abstract— Electrodynamic bearings (EDBs) are passive magnetic bearings that exploit the interaction between eddy currents developed in a rotating conductor and a static magnetic field to generate forces. Similar to other types of magnetic suspensions, EDBs provide contactless support, thus avoiding problems with lubrication, friction and wear. Electrodynamic bearings have also drawbacks such as the difficulty in insuring a stable levitation in a wide speed range. The paper presents a solution where the EDBs are coupled with active magnetic dampers (AMDs) to guarantee a stable levitation.**

## I. ELECTRODYNAMIC LEVITATION OF ROTORS

### A. Introduction

Magnetic levitation of rotors has been an important research subject in the last decades. In addition to the developments on classical active magnetic bearings (AMB), recently, the research on more energy efficient systems associated to the developments on high-strength permanent magnet materials led the scientific community to focus on alternative contactless suspension systems. Usually this is achieved by combining the efforts of permanent magnet bearings (PMB), which are passive, with actively controlled electromagnets.

Examples of systems applying this concept are hybrid magnetic bearings (HMB) and self-bearing motor (SBM) devices. Among these systems, the only one that allows obtaining passive levitation is the PMB. However, since the forces arise from the interaction between magneto-static fields these bearings have a destabilizing stiffness contribution in at least one degree of freedom. An interesting alternative to generate stabilizing forces passively and that can be exploited in the field of magnetic bearings are electrodynamic bearings which have the unique characteristic of producing positive stiffness by passive means without introducing negative stiffness in any direction [1,2]. Despite the promising characteristics of this type of bearings, rotors supported by EDBs are affected by different types of instabilities that must be taken into account.

In the paper a combined EDBs – AMDs configuration is proposed as a possible solution to exploit the high reliability of EDBs overcoming the stability problem by means of

AMDs. It requires studying the effect of the combination of electrodynamic and AMD forces both analytically and experimentally. This is aimed at developing an analytical model of the system taking into account the rotor and the actuators (EDBs and AMDs) characteristics. Furthermore a test rig was designed and built to test experimentally the suspension system.

The proposed hybrid configuration is attractive for high speed magnetically suspended systems because:

- it results in an increased global system reliability
- it allows downsizing the AMBs because the EDBs, for speed above the stability threshold, give a large force contribution for the levitation
- it is possible to discard the traditional ceramic landing bearings because, in case of AMBs failure, the EDBs are able to guarantee a stable levitation until a certain speed, considered safe to land, is reached.

The proposed solution can be considered as a suspension system for high speed applications such as turbomolecular pumps, oil and gas turbines and flywheels for energy storage.

### B. Modeling

The paper presents the model of the complete levitating system composed of a 4 degrees of freedom model of the rotor supported by the combination of electrodynamic suspension with active magnetic dampers, shedding light onto the dynamic behavior of the system. The analytical model supports the design phase and the study of dynamic behavior and stability becomes a key factor for an aware design.

The main assumptions for the model validity are:

- 4 dof rotor, its inertia properties are represented by its mass, its moments of inertia  $J_p$  and  $J_t$ ;
- conductor rigidly mounted on the rotor and its contribution is taken into account in the rotor inertia properties;
- electrical and electromechanical properties of the electrodynamic bearing are isotropic;
- stator part of the electrodynamic bearing rigidly fixed to the case of the machine;
- AMDs non-rotating damping introduced directly on the rotor [3], parameter  $c_n$  shown in Figure 1.

The analytical model of the 4 dof rotor on EDBs refers to the paper “Stability of a 4DOF rotor on electrodynamic passive magnetic bearings” published separately by the Authors in the ISMB14 conference [8]. A detailed description of EDBs analytical model is presented in [4] and the stability issue is deeply described in [5]. The guidelines to design and model the AMDs device can be found in [6].

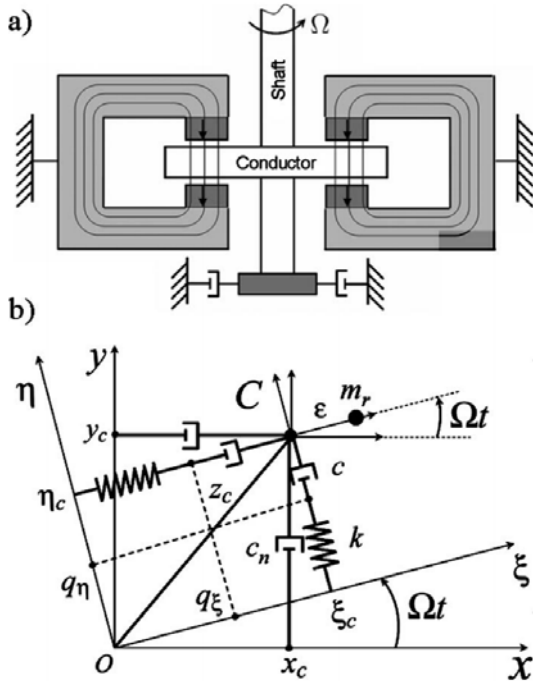


Figure 1: a) scheme of an electrodynamic bearing stabilized by introducing the damping between the rotating part of the bearing and the casing, b) schematization of the equivalent Jeffcott rotor model.

A scheme of a standard EDB suspension system with the introduction of the stabilizing non-rotating damping directly on the rotor is shown in Figure 1 a). Figure 1 b) shows the mechanical equivalent model of a single flux EDB supporting a Jeffcott rotor. The double flux EDB model can be obtained adding, in both directions  $\eta$  and  $\xi$ , a second branch with a damper-spring series in parallel to the one present in the scheme. Therefore the double flux EDB is characterized by the parameters  $k_1, c_1, k_2, c_2$  instead of  $k$  and  $c$ .

The model of each single device considered separately from the others does not represent an innovative contribution to the magnetic levitation topic. By converse, the model which integrates the EDB double flux dynamic model, the AMDs system and the 4 dof model of the rotor gives new contribution to the subject since it allows describing the dynamic behavior of the whole system taking into account the cylindrical and conical instabilities representing a critical aspects of EDBs levitating systems.

Figure 2 shows the scheme of the complete model where the three main blocks represent the EDBs, the AMDs and the rotor. The scheme highlights the connections between the subsystems. Considering a reference frame where the  $z$  axis represents the axial coordinate and the  $x, y$  axes are the radial coordinates, the rotor block receives the forces in  $x$  and  $y$

directions by the EDBs, the AMDs and a generic external disturbance force contribution. The outputs of the rotor block are the  $x$  and  $y$  positions of the shaft referring to the EDBs and AMDs positions (Fig. 3 c). The EDB blocks receive the  $x$  and  $y$  positions and generate the force contribution in the same directions according to the rotating speed that is an input parameter to the whole model. No force in  $z$  direction is produced by the EDBs. The AMD blocks receive the  $x$  and  $y$  positions measured by the sensors and generate a force proportional to the first derivative of the position error to add non-rotating damping contribution to the system.

It must be taken into account that the rotor weight acts on the  $y$  axis.

Figure 3 shows the position of the EDB1, EDB2, AMD1, AMD2 with respect to the center of mass. The values of the parameters  $a_1, a_2, b_1, b_2$  are listed in Table I.

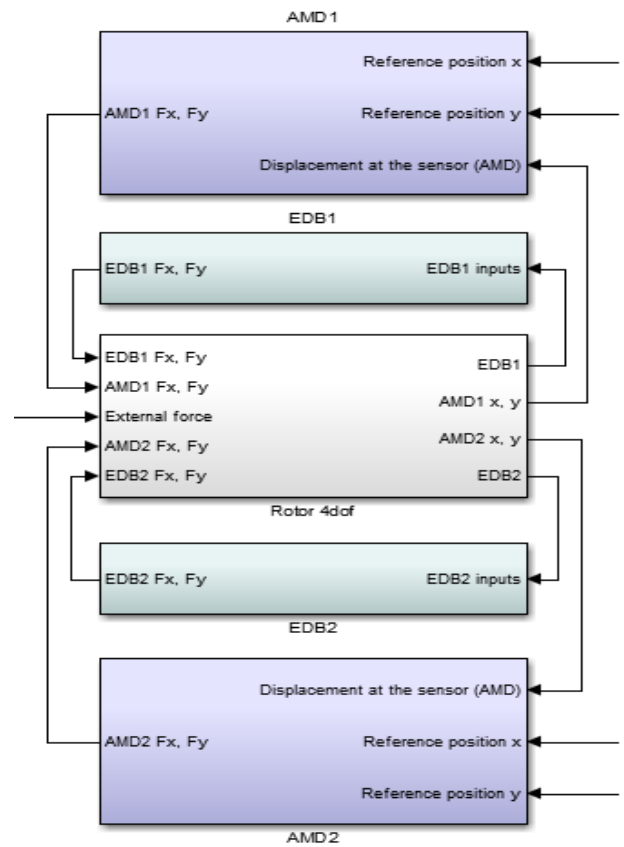


Figure 2: block diagram model of the Hybrid suspension system. AMD1 and EDB1 act on the left-hand side while AMD2 and EDB2 act on the right-hand side

### C. Test Rig

A test rig was designed and built to demonstrate the feasibility of the proposed magnetic suspension and to validate the analytical model. The horizontal axis test rig is shown in Figure 3.

A standard EDB based suspension is characterized by the impossibility of providing levitation forces at zero spin speed and a stiff mechanical connection between the shaft and the basing must be ensured until the stabilization threshold speed

is overcome. By converse, in the proposed solution the AMDs can be used as an active magnetic bearing to guarantee levitation for speed lower than the EDB stability threshold or for speed where the force contribution due to EDBs is not enough to levitate the rotor, and as pure damper for higher speed ensuring a stable levitation for a wide speed range. In this paragraph the mechanical layout of the test rig devised to fulfil the application requirements is presented.

The prototype is composed of four main parts: test rig structure, EDB's statoric magnetic circuit, AMD's stator coils and the rotating shaft. In Figure 3a) the main components of the test rig can be identified while Figure 3b) gives a clearer overview of the whole system. Figure 3c) highlights the rotor properties.

The structure of the test rig is composed by four stainless steel columns (1) connected to three aluminium layers that ensure a stiff construction. The connection of this structure to a seismic mass is done by means of two steel profiles (7). Two structural parts dedicated to the housing of radial position probes used for monitoring are attached to the end plates. These elements host also the supports for the statoric coils of the electromagnets (6) that works as AMBs for low rotating speed and as AMDs when the levitation is provided by EDBs. The stator of the EDB (5) contains four NdFeB N42 magnets oriented in attraction. The magnetic circuit closure is done using two plates of soft iron kept apart by an aluminium structure. The rotating part of the test rig contains a stainless steel shaft to which are attached the copper discs of the EDB (2), the motor's discs (3) and the rotating iron parts of the active actuator. A detailed view of the rotor is shown in Fig.3 c). The electric motor is a brushless axial flux motor and was designed exclusively for this application. The motor uses air wound coils in the stator to reduce the interactions between motor's disc (3) and stator (4), eliminating negative stiffness contributes due to reluctance forces. It will be used for the control of the z direction degree of freedom. The main parameters characterizing the test rig are summarized in Table I.

TABLE I. TEST BENCH PARAMETERS

	Parameter	Value
$\omega$	Nominal speed	20000 rpm
$m_r$	Rotor mass	4.35 kg
$l_r$	Rotor length	305 mm
$J_p$	Polar moment of inertia	0.00572 kg m <sup>2</sup>
$J_t$	Transversal moment of inertia	0.01995 kg m <sup>2</sup>
$g_r$	Radial air gap	0.5 mm
$a_1$	EDB1 arm	67 mm
$a_2$	EDB2 arm	67 mm
$b_1$	AMD1 arm	125 mm
$b_2$	AMD2 arm	125 mm

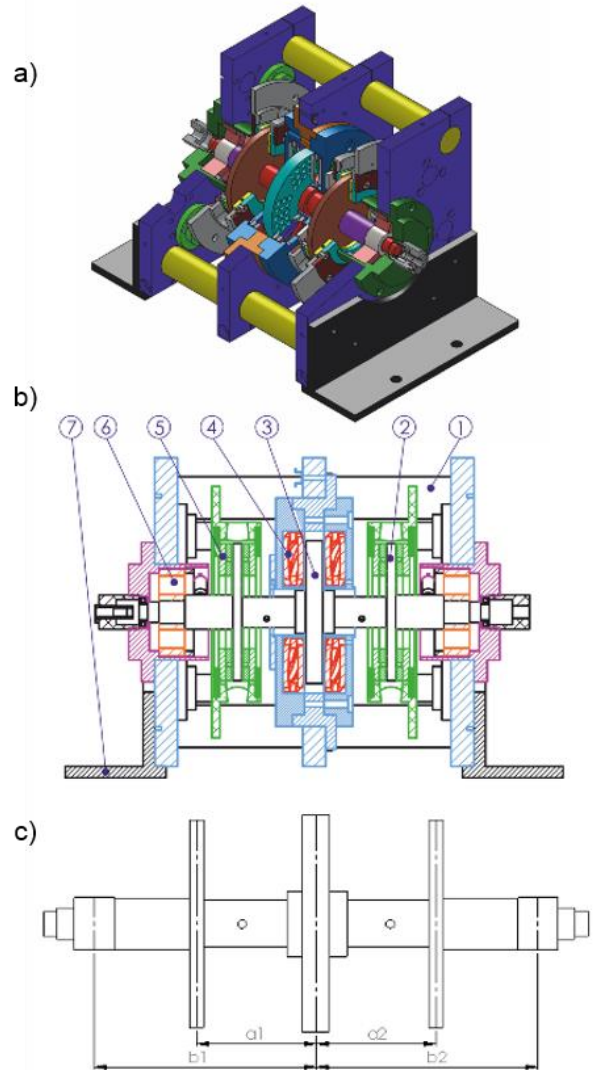


Figure 3 a): isometric section view of the test rig, b), Cross section view, c) rotor view with geometrical parameters.

It is worth to notice that  $J_p < J_t$ , therefore the rotor can be considered as a long rotor. This implies, according to what stated in [8], that both cylindrical and conical modes of a rotor supported by EDBs needs to be stabilized.

The double flux EDBs cross section view containing the main design parameters is shown in Figure 4. The geometry of the EDB has a very important role on its electromechanical properties and must be chosen to respect mechanical constraints and specifications that minimize the rotational speed at which the system becomes stable. To this end the analytical model presented in [4, 5] is used as design tool and the procedure described in [7] is applied. During the design phase the finite element (FE) analysis has a fundamental role to identify the EDB electromechanical performance. The design work flow is characterized by the following steps:

- perform a FE analysis and extract the parameters  $k$  and  $c$
- estimate the total rotor's mass  $m_r$  and EDB's stator mass  $m_s$

- calculate the minimum rotational speed  $\omega$  for which all the poles of the system have negative real part considering a certain range of  $c_n$
- change the geometric parameters and reiterate the previous points until a physically feasible solution that respect's the design constraints is found.

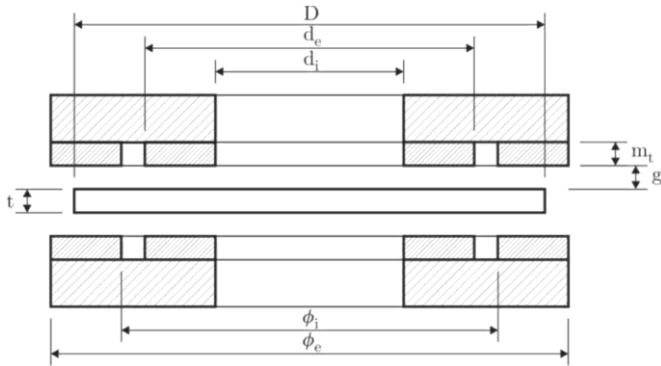


Figure 4: geometry of the axial flux EDB in the double flux configuration.

The list of the EDB parameters coming from the design procedure is presented in Table II.

Parameter	Value
$D$	Conductor outer diameter 120 mm
$d_e$	Inner permanent magnet outer diameter 89 mm
$d_i$	Inner permanent magnet inner diameter 64 mm
$m_t$	Permanent magnet thickness 5.5 mm
$t$	Conductor disc thickness 8 mm
$g$	Axial air gap 0.75 mm
$\Phi_e$	Outer permanent magnet outer diameter 120 mm
$\Phi_i$	Outer permanent magnet outer diameter 95 mm
$B_r$	Residual induction 1.3 T
$\omega_{EDB}$	EDB electric pole 440 rad/s
$k_1$	EDB equivalent stiffness1 129690 N/m
$k_2$	EDB equivalent stiffness2 123979 N/m
$c_1$	EDB equivalent damping1 72.2 Ns/m
$c_2$	EDB equivalent damping2 295.2 Ns/m
$c_n$	Non-rotating damping 500 Ns/m

The  $C_n$  parameter represents the smallest value to get the stability even at zero rotating speed.

The active actuator, devised to levitate the rotor at low speed and stabilize the EDB system, is characterized by the traditional eight poles configuration shown in Fig.5. The actuator working as AMB is designed to support the rotor weight and as AMD to provide the non-rotating damping needed to stabilize the EDB levitation.

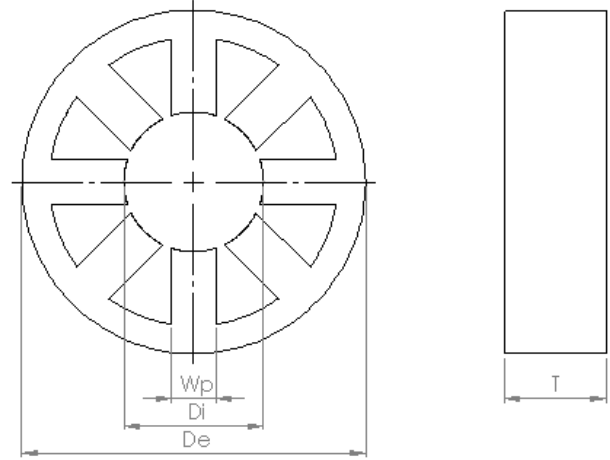


Figure 5: geometry of the AMD actuator.

Table III resumes the main characteristics of the active actuators.

Parameter	Value
$De$	Outer diameter 152 mm
$Di$	Inner diameter 31 mm
$Wp$	Pole width 10 mm
$T$	Actuator thickness 22.5 mm
$N$	Number of turns 165
$Wd$	Wire diameter 0.63 mm
$F$	Actuator force 71 N

The AMD functionality is exploited for low rotating speed, where the EDBs, even if already stable, are not able to generate enough force to levitate the rotor.

#### D. Simulation Results

Simulations have been performed to evaluate the performance of the test rig. Most of the analyses were done considering the operating condition where the levitation is provided by the EDBs and the AMDs give the stabilizing contribution. This is the most critical condition.

The operating condition where the levitation is provided by AMBs is not described since it does not represent an innovative issue.

Figure 6 shows the root loci plot as function of the rotating speed for two values of non-rotating damping  $c_n$ . It is worth to notice that the right choice of  $c_n$  results in a system that is always stable, also for really low rotating speed. This condition is represented by Fig. 6 a) where the roots of the system are on the left hand side of the diagram for the whole range of the operating rotating speed. By converse an inappropriate design of the  $c_n$  parameter brings to an unstable system as shown by Fig. 6 b) where there is at least one pole on the right hand side that never crosses the imaginary axis.

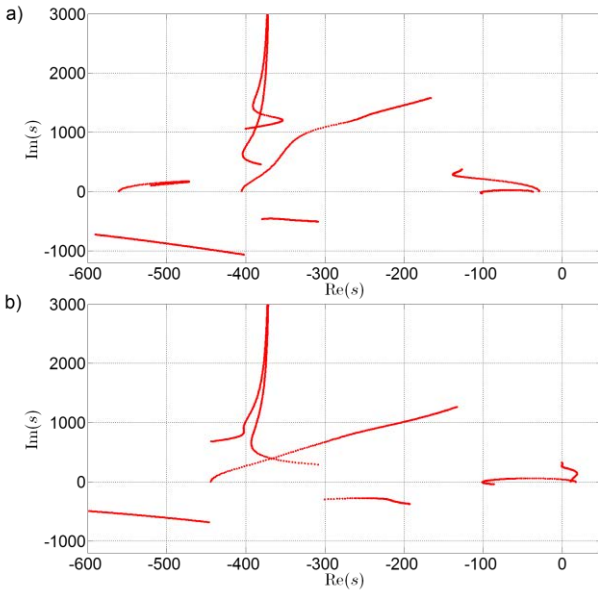


Figure 6: root loci diagram as function of the rotating speed. a)  $c_n = 585$  Ns/m, stable system; b)  $c_n = 455$  Ns/m, unstable system.

The simulations in the time domain are performed considering that the rotor is kept in levitation by means of the AMBs up to a certain rotating speed. Once this speed is reached, the active actuators stop operating as AMBs and start working as AMDs to make possible the electrodynamic levitation. The AMBs levitate the rotor in the equilibrium point  $x = 0, y = 0$  that represents the initial condition for the electrodynamic levitation. The equilibrium point of the rotor supported by EDBs is not fixed and depends on the rotating speed. The main results of the simulations in the time domain are summarized in Fig. 7 and Fig. 8.

Fig. 7 shows rotor radial displacements (x blue, y red) at the left EDB level. Fig. 7 a) and b) refer to a rotational speed  $\omega = 2000$  rpm with non - rotating damping  $c_n = 455$  Ns/m, and  $c_n = 585$  Ns/m respectively in both the AMDs. The results in Fig. 7 c) varies from that in Fig. 7 b) for the higher rotational speed ( $\omega = 8000$  rpm).

According to the root loci plot of Fig. 6 b), the time response of Figure 7 a) shows an unstable behavior that can be observed by the exponential increment of the radial displacements with respect to the time.

The result in Figure 7 b) and c), highlight a stable behavior as the x and y positions reach a constant value. These results are consistent with the root loci plot in Fig. 6b. It must be highlighted that in both cases the position oscillations are contained within the radial air gap and therefore it can be concluded that the EDBs are able to provide enough force to keep the rotor in levitation without any contact with the statoric parts starting from 2000 rpm. Another interesting consideration concerns the different behavior of the system as function of the rotating speed. From the graphs of Figure 7 b) an c) it is possible to note that for rotating speed lower than the EDBs electric pole  $\omega_{EDB}$  (6 b), the x and y positions are larger than the one obtained for higher rotating speed (6 c). This is due to the fact that, according to the quasi-static characteristic of EDB [4], for rotating speed lower than  $\omega_{EDB}$

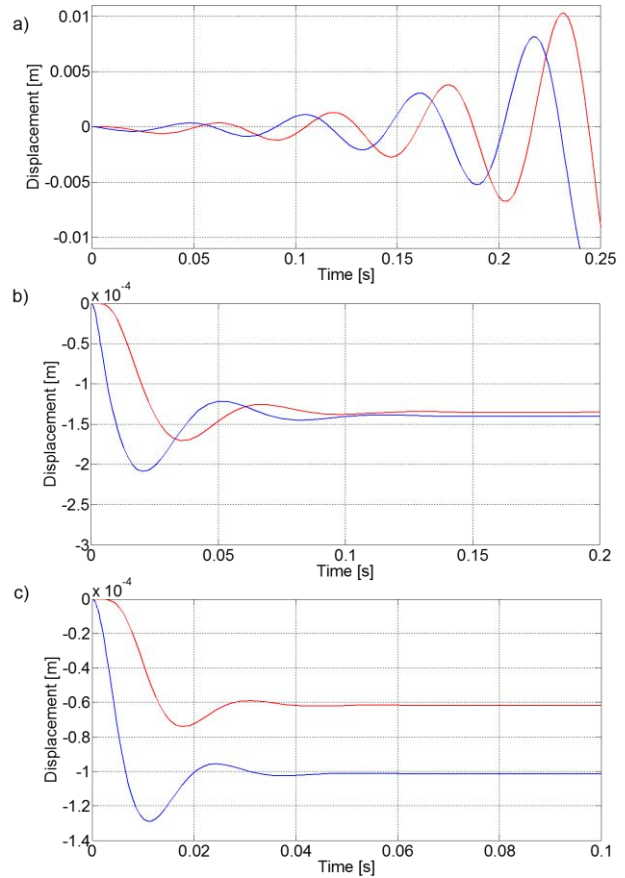


Figure 7: time response of the electrodynamic levitation system stabilized by AMDs. a)  $c_n = 455$  Ns/m, unstable system; b)  $c_n = 585$  Ns/m,  $\omega = 2000$  rpm, stable system; c)  $c_n = 585$  Ns/m,  $\omega = 8000$  rpm, stable system.

the orthogonal force component is larger than the force parallel to the eccentricity, while above  $\omega_{EDB}$  the higher the rotating speed the larger the parallel and the lower the orthogonal component.

Figure 8 describes the rotor orbit under different operating conditions. Graphs a) and b) are obtained with the same  $C_n = 585$  Ns/m that stabilizes the system and describe the behavior at different rotating speed. Also in this graph it can be pointed out that the higher the rotating speed, the smaller the x, y coordinates of the equilibrium point. Figure 8 c) describes the orbit of the system with a  $c_n$  not enough to stabilize the system.

Experimental tests will be performed to validate the analytical model and to get experimental evidence of the advantages of the proposed solution.

### E. Conclusions

The magnetic suspension proposed in the present work is an integrated EDB/AMD solution which exploits the high reliability of EDB with the controllability advantage of the AMD thus eliminating most of the problems due to both technologies.

The proposed solution is attractive for high speed applications because it increases the global system reliability,

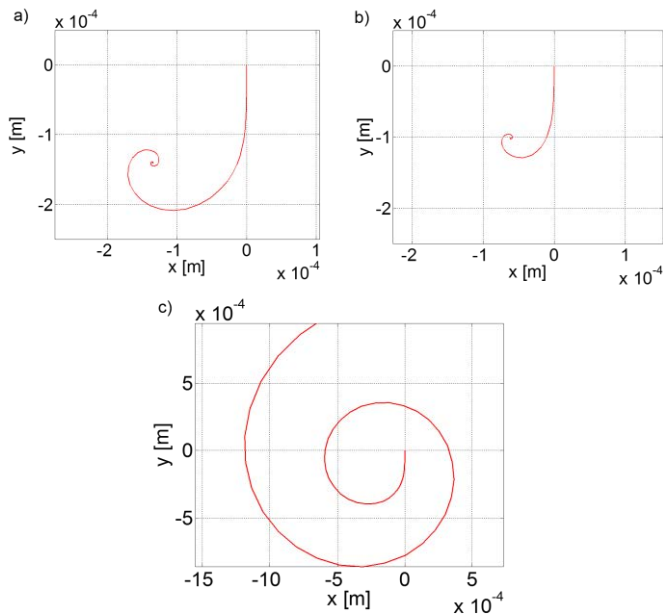


Figure 6 x-y orbit diagram of the electrodynamic levitation system stabilized by AMDs. a)  $c_n = 585$  Ns/m,  $\omega = 2000$  rpm, stable system; b)  $c_n = 585$  Ns/m,  $\omega = 8000$  rpm, stable system; c)  $c_n = 445$  Ns/m, unstable system.

makes possible an AMB downsizing and represents an alternative to the landing bearing problem.

The analytical model of the suspension system with a 4 degrees of freedom rotor was developed and used to design a test rig.

The simulation results shed light onto the promising characteristics of the hybrid EDB/AMD suspension.

Experimental tests will be performed to validate experimentally what observed in simulation.

#### REFERENCES

- [1] P. A. Basore. Passive stabilization of flywheel magnetic bearings. Master's Thesis, Massachusetts Institute of Technology, Cambridge, USA, 1980.
- [2] J. G. Detoni, "Progress on electrodynamic passive magnetic bearings for rotor levitation," Proceedings of the Institution of Mechanical Engineers, Part C: Journal of Mechanical Engineering Science, 2013, doi:10.1177/0954406213511798.
- [3] A., Filatov, 2006, "Flywheel Energy Storage System With Homopolar Electrodynamic Magnetic Bearing," Proceedings of the Tenth International Symposium on Magnetic Bearings, Martigny, Switzerland.
- [4] Amati, N., De Lépine, X., and Tonoli, A., 2008, "Modeling of Electrodynamic Bearing," ASME J. Vibr. Acoust., 130, p. 061007.
- [5] A. Tonoli, N. Amati, F. Impinna, and J. G. Detoni, "A solution for the stabilization of electrodynamic bearings: Modeling and experimental validation," Journal of Vibrations and Acoustics, vol. 133, no. 021004, 2011.
- [6] G. Schweitzer, H. Bleuler and A. Traxler. "Active Magnetic Bearings: Basics, Properties and Applications of Active Magnetic Bearings" vdf Hochschulverlag an der ETHZ, Zurich, 1994.
- [7] N. Amati, J.G. Detoni, F. Impinna, A. Tonoli, "Model Based Design of a Rotor Supported by Radial Electrodynamic Bearings". 10th International Conference on Vibrations in Rotating Machinery, Londra, 11-13 September, 2012. pp. 123-132

- [8] J. D. Detoni, F. Impinna, N. Amati, A. Tonoli, M.P. Piccolo, "Stability of a 4DOF rotor on electrodynamic passive magnetic bearings", 14<sup>th</sup> International Symposium on Magnetic Bearings, Linz, 11-14 August, 2014.